

Distributed three-dimensional fiber Bragg grating refractometer for biochemical sensing

S. Keren and M. Horowitz

Department of Electrical Engineering, Technion—Israel Institute of Technology, Haifa 32000, Israel

Received May 15, 2003

We demonstrate a three-dimensional (3-D) distributed refractometer that measures refractive index in a small volume. The sensor is based on an evanescent-wave fiber Bragg grating that is interrogated by low-coherence spectral interferometry. The measurement can be performed on a short time scale without the need for a mechanical scan. The new sensor was used to simultaneously measure glucose concentration in several droplets along a single sensor and to interrogate the time-dependent evaporation process of a water droplet. The new measurement technique might enable novel 3-D distributed sensors to be developed and multiple discrete measurements to be made in a small volume. © 2003 Optical Society of America

OCIS codes: 060.2370, 290.3030, 050.2770.

Optical fiber evanescent-wave biochemical sensors are miniature, low-cost, reliable, sensitive, and versatile. Therefore such sensors became important in various applications such as environmental monitoring, chemical and biochemical measurements, and drug development.^{1–3} Optical fibers are also attractive for performing *in vivo* medical biochemical measurements because fibers are small and flexible enough to be inserted inside thin needles and are nontoxic, chemically inert, and intrinsically safe for the patient. Several methods have been demonstrated for obtaining evanescent-wave refractive-index sensors.^{4–6} However, in all of them the average refractive index was measured along the whole active sensor element, limiting the spatial resolution that could be obtained. In this Letter we demonstrate, for the first time to our knowledge, a distributed biochemical evanescent-wave fiber Bragg sensor. The evanescent-wave sensor can measure the refractive index of the medium surrounding the fiber along a fiber length of a few centimeters with a spatial resolution of the order of tens of micrometers. Such high-resolution distributed measurements are needed for investigating several important phenomena such as the propagation of a liquid droplet on a glass surface, propagation of electrical pulses in biological cell clusters, and growth of biological cells. The new measurement technique may also be important for gauging the performance of several biochemical tests in a single sensor with a small volume.

Recently we and our colleagues demonstrated a one-dimensional distributed temperature sensor for measuring temperature profiles in high-power optical fiber components.⁷ The temperature profile was measured along an optical fiber Bragg grating with a resolution of the order of tens of micrometers by low-coherence interferometry performed in the spectral domain. The measurement technique does not require a slow mechanical scan. A distributed one-dimensional fiber sensor can also be interrogated by use of a tunable laser⁸ or of low-coherence reflectometry.⁹ The use of an evanescent wave in a sensor limits the interrogated region to a small volume.

In this Letter we demonstrate, for the first time to our knowledge, a three-dimensional (3-D) distributed refractometer that measures the refractive index in a small volume. The sensor is based on an evanescent-wave fiber Bragg grating that is interrogated by low-coherence spectral interferometry.¹⁰ Figure 1 shows a schematic illustration of the sensor. The sensor is based on a D-shaped fiber (D-fiber) with a core located close to the flat surface of the fiber. The interrogated volume is determined by the profile of the field outside the fiber. The volume is limited in one of the directions to a length scale of the order of a few micrometers because of the limited penetration depth of the evanescent field. In the second direction the interrogated volume is limited to a length scale of $\sim 10 \mu\text{m}$ by the mode-field diameter of the fiber. In the third direction the interrogated volume is limited to a length scale of the order of tens of micrometers by the resolution of the low-coherence tomography technique that is used to extract the grating parameters. The measurement of the refractive index can be performed on a short time scale without the need for a mechanical scan.¹⁰ The short time scale of the measurement might be important in studies of dynamic effects, such as the propagation of a droplet on a surface. We have demonstrated in the research reported here the simultaneous measurement of the

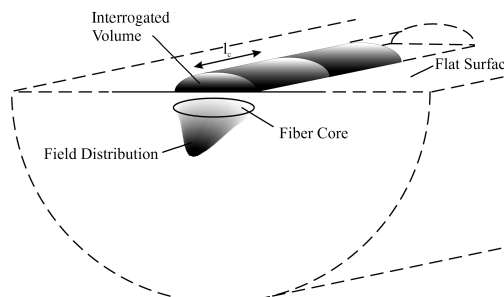


Fig. 1. Schematic description of a 3-D distributed evanescent-field fiber Bragg sensor. The interrogated volume is bounded by the penetration depth of the evanescent field, the mode-field diameter, and the coherence length of the measurement, l_c .

glucose concentration in four droplets along a single sensor. We have also demonstrated a measurement of the time-dependent evaporation process of a water droplet. This new measurement technique might facilitate the development of novel 3-D distributed sensors and enable multiple discrete measurements to be performed in a small volume.

Our new sensor was based on a grating written in a D-fiber. We wrote a uniform fiber Bragg grating with a central wavelength of ~ 1542 nm in a hydrogen-loaded optical D-fiber by illuminating the fiber with an UV laser beam by means of a phase mask. The maximum reflection coefficient of the grating was $\sim 20\%$. After writing the grating, we etched the D-fiber to obtain a significant evanescent field. Previously it was shown that the smoothness of the etched fiber surface depends on the etchant's composition.¹¹ We obtained a sufficiently uniform sensor by using a buffered HF etchant with the following composition (volume ratio): 40% $\text{NH}_4\text{F}:\text{H}_2\text{O}:49\%$ HF = 62.5:33.3:4.2, and with an etch rate of ~ 40 nm/min. We performed *in situ* monitoring of the etching process by measuring the Bragg wavelength shift of the reflected wave from the grating that was due to the evanescent wave. We stopped the etching when the Bragg wavelength shift was equal to $\delta\lambda = 2.4$ nm. Figure 2(a) shows a schematic cross section and a zoom in on the elliptical core of the D-shaped fiber that had a germanium-doped core, a fluorine-doped inner cladding, and a silica outer cladding. Figure 2(b) shows a scanning electron microscope cross-section image of the D-fiber's facet after etching and a zoom in on the core region. Inasmuch as different fiber regions are affected slightly differently by etching, the figure shows a clear image of the fiber structure.

The parameters of the grating were interrogated by low-coherence spectral interferometry.¹⁰ The low-coherence light source was a broadband fiber laser that operated in a noiselike mode of operation¹² and generated linearly polarized pulses with a bandwidth of 70 nm around a wavelength of 1550 nm. The birefringence of the D-fiber caused the two polarization modes of the fiber to have different Bragg wavelengths. In our measurement we aligned the input polarization state with one of the principal axes of the D-fiber. We achieved polarization alignment by minimizing the intensity of the reflection peak in the spectrum that was caused by one of the polarization components. The interference spectrum of pulses reflected from the grating and pulses reflected from a reference mirror was measured with an optical spectrum analyzer. The impulse response of the grating, $h(t)$, was obtained by use of an inverse Fourier transform of the interference spectrum.¹⁰ The spatial resolution of the low-coherence spectral interferometry measurement technique is determined by the minimum bandwidth of the laser and the grating. For a light source with a bandwidth of 70 nm the spatial resolution can be as short as $\delta z \approx 10$ μm . Consequently such a measurement technique theoretically can separate ~ 5000 locations in a single sensor element with a length of 5 cm.

Strong coupling between the two counterpropagating waves in a fiber Bragg grating is obtained when the Bragg condition is met. The Bragg condition is highly sensitive to changes in the effective refractive index, n_{eff} . Therefore a variation in the refractive index of the medium surrounding the fiber changes the Bragg wavelength because of presence of an evanescent wave. In our experiment the maximum reflection of the grating was low ($\sim 20\%$), and therefore the first-order Born approximation could be accurately used.⁷ In the first-order Born approximation, the phase of the impulse response directly gives the change in the effective refractive index:

$$\frac{d\{\arg[h(z)]\}}{dz} = \frac{d\{\arg[q(z/2)]\}}{dz} - \frac{4\pi}{\lambda_B} \delta n_{\text{eff}}(z/2), \quad (1)$$

where $q(z)$ gives the parameters of the grating before the interrogated medium was placed on the fiber¹³ and δn_{eff} is the change in the effective refractive index that is due to the medium surrounding the grating. We neglect changes in the refractive-index amplitude that are due to the evanescent wave, because the grating is written mainly in the fiber's core. We also neglect the absorption that is due to the evanescent wave.

We performed two experiments to demonstrate the high spatial resolution and the time-dependent capability of the new 3-D distributed evanescent-wave sensor. In the first experiment we placed four liquid droplets with different refractive indices on the same fiber sensor. The first droplet was distilled water, and the other three droplets contained D-glucose solutions with concentrations of 1, 2, 3 moles of solute per liter of solution (M). The grating length was ~ 9 mm, the sizes of the droplets were 1–2 mm, and the spacing between the droplets was ~ 1 mm. We measured and subtracted the extracted effective refractive index before and after adding the droplets. Figure 3 shows the extracted effective refractive-index change caused by adding the droplets. Each step in the refractive-index profile was caused by a different droplet. The experimental results show that the effective refractive index increased as the glucose concentration grew, as expected.

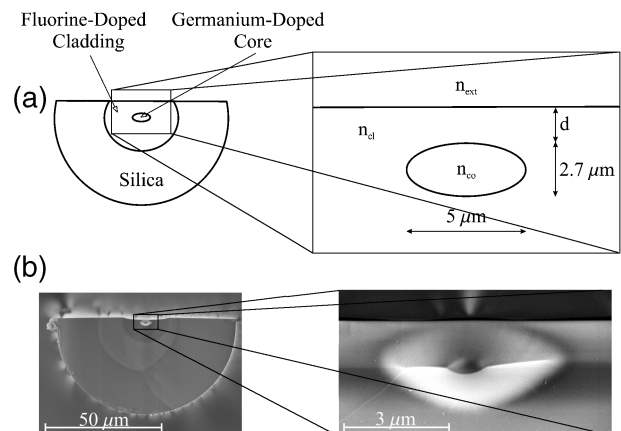


Fig. 2. (a) Schematic description and (b) a measured scanning electron microscope image of the fiber sensor cross section.

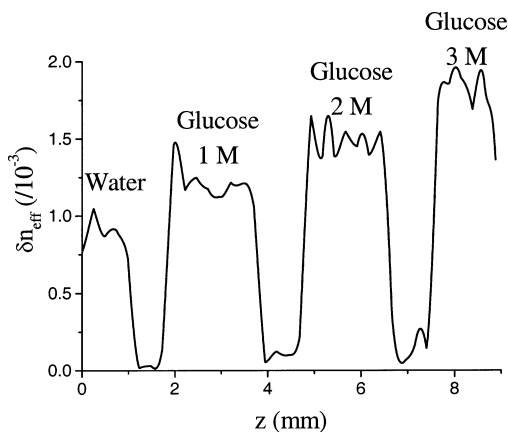


Fig. 3. Measurement of the effective refractive-index change caused by placement of four droplets with different concentrations of glucose on the same fiber sensor.

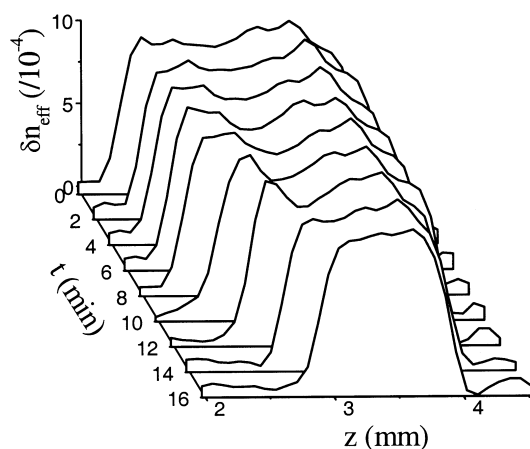


Fig. 4. Evaporation of a water droplet as a function of time. The droplet shrank through evaporation from ~ 1.8 to ~ 1 mm after 16 min. After ~ 18 min the droplet disappeared.

In the second experiment we measured the evaporation of a water droplet. We placed a distilled-water droplet on the sensor and measured the refractive-index profile every 2 min. Figure 4 shows that the droplet shrank through evaporation from ~ 1.8 to ~ 1 mm after 16 min. After ~ 18 min the droplet disappeared, and only a small amount of noise was measured. The measured interference spectrum bandwidth was 10 nm, and therefore the spatial resolution was $\sim 70 \mu\text{m}$. Because our measurement technique does not require a mechanical scan, the time resolution between measurements can be much shorter than demonstrated.

Theoretically, the minimum detectable phase change in the impulse-response function is limited by the wavelength resolution of the spectrum analyzer that measures the interference pattern. In practice, the resolution is limited by noise added in the measurement. The accumulated phase of the impulse response depends linearly on the length of the interrogated region, and therefore the sensitivity of the measurement is inversely proportional to the

spatial resolution. In our measurements the phase noise was equivalent to a change in the effective refractive index of $n_{\text{eff}} = 4 \times 10^{-5}$ when the spatial resolution was $\sim 70 \mu\text{m}$. A conversion of the effective refractive-index resolution into the minimum-detectable change in the external refractive index depends on the fiber parameters and on the refractive index of the surrounding medium. We calculated the dependence of the effective refractive index of the fiber on the external refractive index, n_{ext} , for the fiber shown in Fig. 2, using the finite-difference method.¹⁴ Assuming that the refractive index of the medium surrounding the fiber is close to the refractive index of water, the minimal detectable change in the external refractive index is $\sim n_{\text{ext}} \cong 4 \times 10^{-3}$ when the spatial resolution equals $70 \mu\text{m}$. We believe that better sensitivity can be achieved by proper thermal and acoustic isolation of the interferometer used in our measurement. In addition, we expect to increase the sensitivity by a factor of 10 by coating the flat surface of the fiber with a thin high-refractive-index layer.

The authors thank Boris Levit for writing the gratings, Otilia Haim for preparing the silica solvent, and Kinneret Keren for helping with the scanning-electron microscopy. The research was supported by the Division for Research Funds of the Israeli Ministry of Science. M. Horowitz's e-mail address is horowitz@ee.technion.ac.il.

References

1. J. P. Moore, B. A. Childers, M. E. Froggat, A. L. Cook, N. C. Coffet, L. J. Coen, J. K. Diamond, P. T. Huynh, E. M. Riley, S. K. Stover, K. G. Vipavetz, J. E. Wells, K. L. Woodman, C. D. Armstrong, J. S. Sirkis, and Y. T. Peng, in *Bragg Gratings, Photosensitivity, and Poling in Glass Waveguides*, Vol. 33 of OSA Trends in Optics and Photonics Series (Optical Society of America, Washington, D.C., 2000), p. 43.
2. T. O'Brien, L. H. Johnson III, J. L. Aldrich, S. G. Allen, L. T. Liang, A. L. Plummer, S. J. Krak, and A. A. Bioarski, *Biosens. Bioelectron.* **14**, 815 (2000).
3. E. Brynda, M. Houska, A. Brandenburg, and A. Wikerstal, *Biosens. Bioelectron.* **17**, 665 (2002).
4. R. Slavik, J. Homola, J. Ctyroky, and E. Brynda, *Sens. Actuators B* **74**, 106 (2001).
5. T. Allsop, L. Zhang, and I. Bennion, *Opt. Commun.* **191**, 181 (2001).
6. K. Schroeder, W. Ecke, R. Mueller, R. Willsch, and A. Andreev, *Meas. Sci. Technol.* **12**, 757 (2001).
7. V. Goloborodko, S. Keren, A. Rosenthal, B. Levit, and M. Horowitz, *Appl. Opt.* **42**, 2284 (2003).
8. S. Huang, M. M. Ohn, M. Leblanc, and R. M. Measures, *Smart Mater. Struct.* **7**, 248 (1998).
9. M. Volanthen, H. Geiger, and J. P. Dakin, *J. Lightwave Technol.* **15**, 2076 (1997).
10. S. Keren and M. Horowitz, *Opt. Lett.* **26**, 328 (2001).
11. R. G. Hiedeman, R. P. H. Kooyman, and J. Greve, *Sens. Actuators B* **12**, 205 (1993).
12. M. Horowitz, Y. Barad, and Y. Silberberg, *Opt. Lett.* **22**, 799 (1997).
13. T. Erdogan, *J. Lightwave Technol.* **15**, 1277 (1997).
14. F. A. Muhammad and G. Stewart, *Int. J. Optoelectron.* **7**, 705 (1992).